Time Dependent Schrödinger Equation

Jackson Burzynski, Caleb Helbling, Justin Lee

April 13, 2015

Abstract

In this project, we have analyzed the solutions to the Time Dependent Schödinger Equation obtained through the finite difference scheme. Two different methods have been implemented and the results from each algorithm are compared. For simplicity, in this project we let $\hbar = m = \omega = 1$. This report contains heatmap plots of the amplitude vs time of the solutions to the TDSE, but we encourage the reader to run our code through the GUI to see the solutions animated.

1 Free Particle

1.1 Comparing Methods

In this project, we have implemented two different finite difference schemes. The first uses the "obvious" finite difference scheme below

$$-\left[\frac{\Psi_{j+1}^{n+1} - 2\Psi_j^{n+1} + \Psi_{j-1}^{n+1}}{(\Delta x)^2}\right] + V_j\Psi_j^{n+1} = i\left[\frac{\Psi_j^{n+1} + \Psi_j^n}{\Delta t}\right] \tag{1}$$

This algorithm is unconditionally stable, however it is non-unitary, so we must normalize the wavefunction at every time step. The second uses a slightly modified approach. This method is superior because it is both stable and unitary. This method uses the equation

$$(1 + \frac{1}{2}iH\Delta t)\psi_j^{n+1} = (1 - \frac{1}{2}iH\Delta t)\psi_j^n \tag{2}$$

So rather than having the equation $A\psi_j^{n+1} = \psi_j^n$ as we did in the first method, we now have $A\psi_j^{n+1} = B\psi_j^n$ where A and B are both tridiagonal matrices. In the following sections we will show how the second method is superior to the first.

1.2 Periodic Boundary Conditions

By applying periodic boundary conditions, we see the particle exit the frame on the right and reappear on the left, as expected. The results from the two different algorithms are shown in Figure 1. Notice how the first algorithm gives undesireable results, such as dissipation and a non-constant velocity of the wavepacket. The second algorithm, however, gives the expected results.

1.3 Zero Boundary Conditions

By applying zero boundary conditions, we effectively place the particle in the infinite square well. For an analysis of this scenario, please see the following section.

2 Common Potentials

2.1 Infinite Square Well

We first look at the classic infinite square well potential. This potential is of the form,

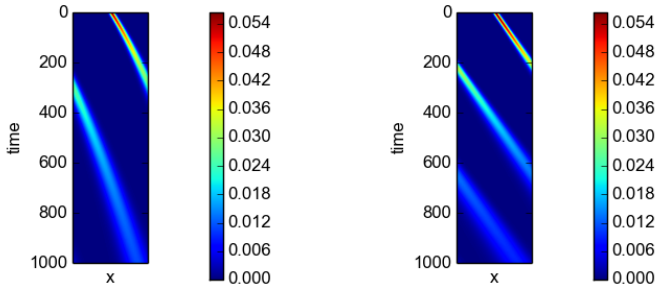

(a) Algorithm 1 (b) Algorithm 2

Figure 1: Free particle with periodic boundary conditions

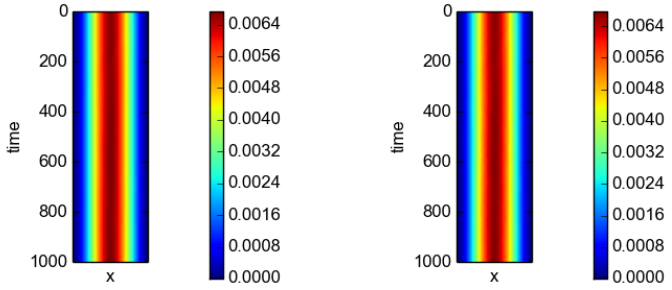

(a) Algorithm 1 (b) Algorithm 2

Figure 2: Ground state of the infinite square well

$$V(x) = \begin{cases} 0 & : -\frac{a}{2} \leq x \leq \frac{a}{2} \\ \infty & : x < -L, x > L \end{cases}$$

The eigenvalues for a particle in the infinite square well are

$$E_n = \frac{n^2\pi^2\hbar^2}{2ma^2} = \frac{n^2\pi^2}{2a^2} \tag{3}$$

with corresponding eigenfunctions

$$\psi_n(x) = \sqrt{\frac{2}{a}} \cos\left(\frac{n\pi}{a}x\right) \tag{4}$$

The first and second eigenstates for both algorihms are shown in Figures 2 and 3. For this potential, the two algorithms gave the same output. Note that the eigenstates do not evolve in time, as expected. For this potential we observe states with the correct energy eigenvalues.

2.2 Harmonic Oscillator

Recall that the potential energy of the harmonic oscillator is of the form

$$V(x) = \frac{1}{2}m\omega^2x^2 \tag{5}$$

For simplicity, we let $m = \omega = 1$, so $V(x) = 1/2x^2$. The eigenvalues for a particle in this potential are

$$E_n = \left(n + \frac{1}{2}\right)\hbar\omega = \left(n + \frac{1}{2}\right) \tag{6}$$

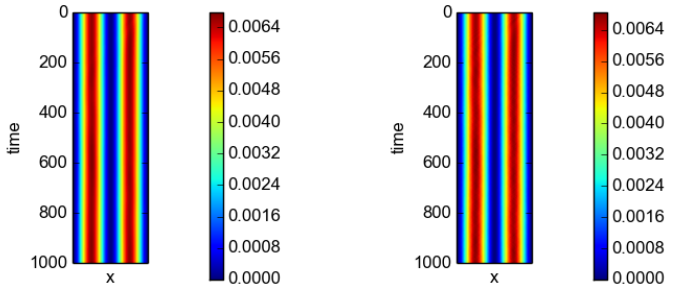

(a) Algorithm 1 (b) Algorithm 2

Figure 3: First excited state of the infinite square well

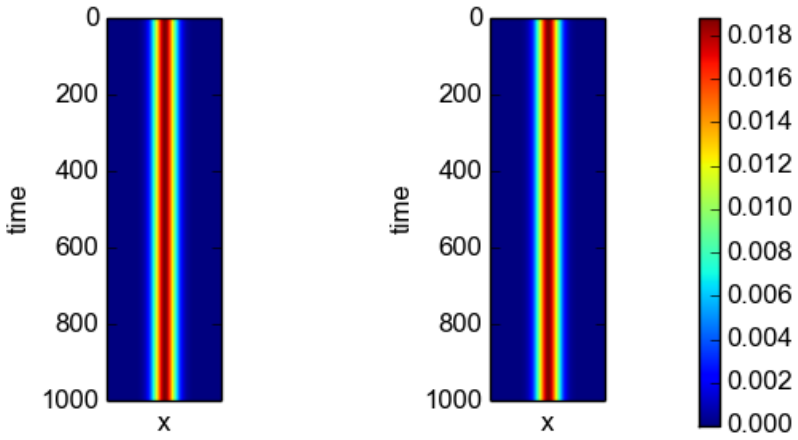

(a) Algorithm 1 (b) Algorithm 2

Figure 4: Ground state of the harmonic oscillator

with corresponding eigenfunctions

$$\psi_n(x) = \left(\frac{m\omega}{\pi\hbar}\right)^{1/4} \frac{1}{\sqrt{2^n n!}} H_n(x) e^{-x^2/2} \tag{7}$$

where $H_n(x)$ is the n^{th} Hermite Polynomial. The plots of the first two eigenstates form both algorithms are shown in Figure 4 and 5 Again note that the eigenstates are stationary in time, as expected. Also notice how the maximum amplitude of the oscillations decreases throughout time in the first algortihm, and stays constant in the second. Again we observe states with the correct energy eigenvalues.

3 Barrier Potential

We now look at a potential barrier. In order to examine how a particle will interact with a barrier, we must multiply our initial gaussian wavepacket by e^{ikx} which results in a gaussian wave packet moving to the right. In this section and those that follow, we will restrict our analysis to the superior finite difference scheme. Figure 6 shows a wavepacket colliding with barriers of different energies. Notice how when $E = 3V/4$, some of the wavepacket is still transmitted. Classically, this scenario is forbidden. In quantum mechanics, however, this process is allowed and is known as *tunneling*.

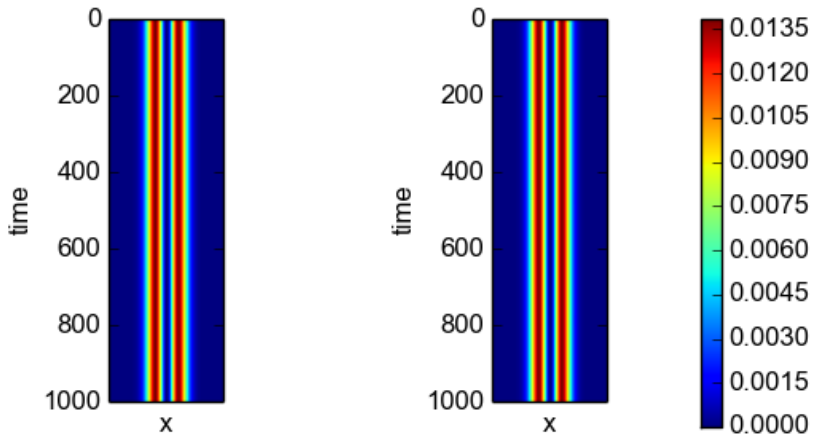

(a) Algorithm 1 (b) Algorithm 2

Figure 5: First excited state of the harmonic oscillator

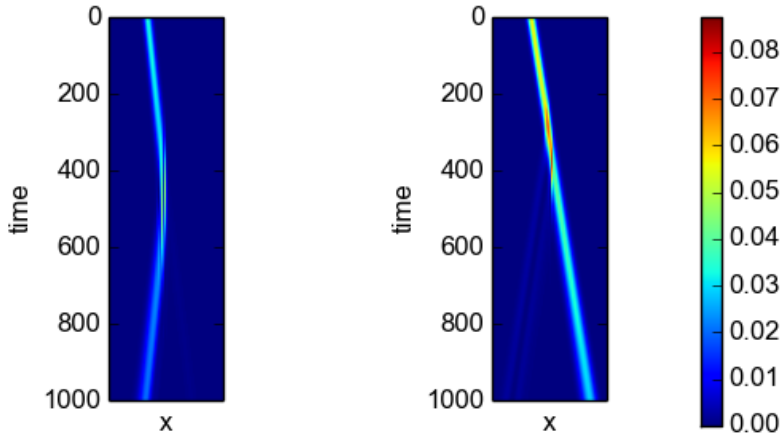

(a) E = 3V/4 (b) E = 2V

Figure 6: Barrier Potential

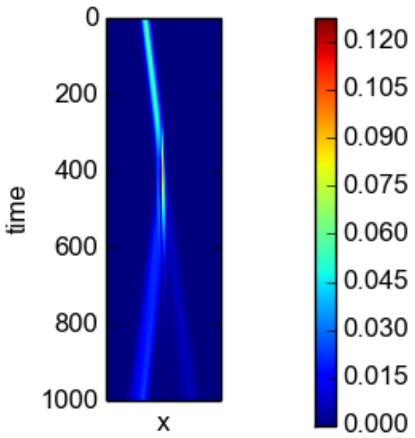

Figure 7: E = V

3.1 Transmition and Reflection Coefficients

Analytically, we expect the reflection and transmission coefficients to be of the form

$$T = \frac{4k_0k_1e^{-ia(k_0-k_1)}}{(k_0+k_1)^2 - e^{2iak_1}(k_0-k1)^2} \qquad R = \frac{(k_0^2-k_1^2)\sin(ak_1)}{2ik_0k_1\cos(ak_1) + (k_0^2+k_1^2)\sin(ak_1)} \tag{8}$$

where $k_0 = \sqrt{2mE/\hbar^2} = \sqrt{2E}$ and $k_1 = \sqrt{2m(E-V)/\hbar^2} = \sqrt{2(E-V)}$. Letting $E = 100$ and $V = 200$, we calculate that $T = 3.9125 \times 10^{-11}$. From the formula above we expect T to be 2.0814×10^{-12}. Thus our results seem relatively consistent.

3.2 Incident Energy Equal to the Barrier Height

We now look at the situation in which the incident energy E equals the height of the potential barrier V. In this situation, we have that $k_1 = 0$, so the transmission and reflection coefficients take a different form. We now have that

$$T = \frac{1}{1 + ma^2V/2\hbar^2} \tag{9}$$

For $E = V = 100$ and $a = 1.0$, our program gives us $T = .002627$. However, from the analytical expression we expect that $T = .01961$. Possible reasons for this discrepency are the equations used for the free particle wavepacket. The analytical calculation uses a piecewise superposition of waves

$$\begin{aligned} \psi_L &= A_re^{ik_0x} + A_le^{-ik_0x} \qquad x < 0 \\ \psi_C &= B_re^{ik_1x} + B_le^{-ik_1x} \qquad 0 < x < a \\ \psi_R &= C_re^{ik_0x} + C_le^{-ik_0x} \qquad x > a \end{aligned}$$

However, we were unable to implement such a wavefunction that gave us meaningful results. Our program uses a simple gaussian multiplied by the time evolution operator

$$\psi = Ae^{ikx - x^2/2} \tag{10}$$

In further analysis, we hope to implement a traveling wave that is consistent with the one used in the analytical calculation to allow a more thorough analysis of the accuracy of our method.

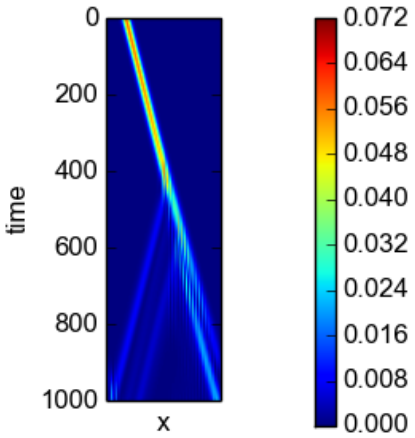

Figure 8: Particle with E = 50 hitting a Kronig-Penny crystal of depth V = -25 and width = 0.4

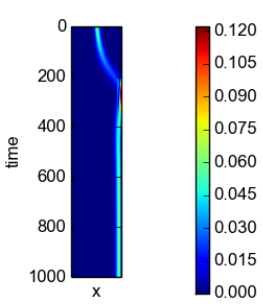

(a) Stationary Gaussian

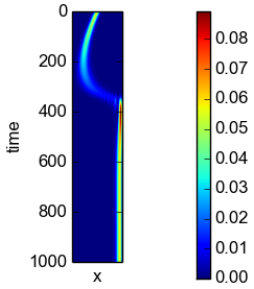

(b) Gaussian moving to the right with E = 20

Figure 9: Complex Potential

4 Kronig-Penney Crystal

The next potential that we looked at was a periodic array of potential wells, i.e. a Kronig-Penny crystal. The heatmap of this scenario is shown in Figure 8. We encourage the reader to experiment with the GUI to look at a wider range of crystal depths and widths.

5 Non-Hermition Hamiltonian

We now look at the potential

$$V(x) = \begin{cases} ix & : -L < x < L \\ \infty & : x \leq -L, x \geq L \end{cases}$$

Although this potential yields a Hamiltonian that is non-Hermitian, it does have real eigenvalues. We were unable to find the eigenstates of this potential, but we were able to obtain some fairly interesting results, as shown in Figure 9. For this potential, even the unitary method did not conserve probability, so we needed to normalize the wavefunction at each step. Notice how the wavefunction is attracted to the "top" of the potential located on the right-hand side of the well.